Electronic Supplementary Material (ESI) for Chemical Science.
This journal is © The Royal Society of Chemistry 2020

Site-Specific Growth of MOF-on-MOF Heterostructures with Controllable Nano-Architectures: Beyond the Combination of MOF Analogues

Chao Liu,[a] Lina Lin,[b] Qiang Sun,[c] Jing Wang,[a] Rong Huang,[b] Wenyi Chen,[a] Shumin Li,[a] Jingjing Wan,*[a] Jin Zou,*[c, d] Chengzhong Yu*[a, e]

[a]School of Chemistry and Molecular Engineering, East China Normal University, Shanghai 200241, P. R. China.

[b]Key Laboratory of Polar Materials and Devices (MOE), Department of electronics, East China Normal University Shanghai 200241, P. R. China.

[c]Materials Engineering, University of Queensland, Brisbane, Queensland 4072, Australia

[d]Centre for Microscopy and Microanalysis, University of Queensland, Brisbane, Queensland 4072, Australia

[e]Australian Institute for Bioengineering and Nanotechnology, The University of Queensland, Brisbane, Queensland 4072, Australia

Methods

Chemicals

Titanium(IV) isopropoxide (TPOT, 97%, Aldrich), (99.5%, Sinopharm Chemical Regent Co., Ltd), aminoterephthalate (99%, Aldrich), Zinc nitrate hexahydrate ($Zn(NO_3)_2 \cdot 6H_2O$, 98%, Sinopharm Chemical Regent Co., Ltd), 2-methylimidazole (2-MeIM, Aldrich), N,N-Dimethylformamide (DMF, 99%, Greagent), methanol (AR), Millipore water were used in all experiments.

Synthesis of $_c$MIL-125

The cake-like $_c$MIL-125 nanoparticles were prepared according to a previous report with a slight modification [S1]. Briefly, 0.6 mL of TPOT and 0.56 g of aminoterephthalate were dissolved into 40 mL mixture of DMF and CH_3OH (9:1, v/v). The mixture was transferred to a 100 mL Teflon-line autoclave and heated at 150 ^oC for 24h before stirring for 5 min. Then, the yellow solid product was collected by washing with DMF and methanol for 3 times. Finally, the as-synthesized $_c$MIL-125 was dispersed in 30 mL methanol for further use. The concentration of $_c$MIL-125 stock solution was determined to be ~ 20 g/L.

Synthesis of $_c$MIL-125@ZIF-8 heterostructure

To synthesize $_c$MIL-125@ZIF-8 heterostructure, 0.1 mL of $_c$MIL-125 suspension (~ 2 mg of $_c$MIL-125), 3 mL of 25 mM 2-MIM solution and 5 ml of 25 mM $Zn(NO_3)_2 \cdot 6H_2O$ solution are mixed and then allowed to react at room temperature for 4 h. The product is then collected by centrifugation, washed with methanol several times, and dried overnight.

Synthesis of $_b$MIL-125

The synthesis procedure of $_b$MIL-125 was also synthesized by a reported method [S2]. A solution prepared by dissolving 0.7 mL of TPOT and 0.86 g of aminoterephthalate in 40 mL mixture of DMF and CH_3OH (1:1, v/v) was transferred to a 100 mL Teflon-line autoclave and heated at 150 ^oC for 15h. Then, the yellow samples were collected by washing with DMF and methanol for 3 times. The as-synthesized $_b$MIL-125 was dispersed in 40 mL methanol for further use.

Synthesis of $_b$MIL-125@ZIF-8 heterostructure

The synthesis process of $_{b}$MIL-125@ZIF-8 heterostructure was similar with $_{c}$MIL-125@ZIF-8 except using $_{b}$MIL-125 as the seed.

Synthesis of ZIF-8

The synthesis process of ZIF-8 was similar with $_{c}$MIL-125@ZIF-8 except without adding MIL-125 using methanol as the solvent.

Material characterization. Transmission electron microscopy (TEM) images were obtained with Hitachi HT7700 at 120 KV. HRTEM observations were carried out using a JEM-2100F (JEOL, Japan) operating at 200 kV equipped with an X-ray energy dispersive spectrometer (EDS: X-Max 80T, Oxford, UK) for chemical composition analyses. X-ray diffraction (XRD) patterns were recorded using a Bruker D8 Advanced X-Ray Diffractometer with Cu Kα radiation (λ=0.154 nm). Fourier transform infrared (FT-IR) spectra of samples were obtained by using FT-IR-Nicolet IS-10 Thermo Fisher. To determine the Ti/Zn contents, all samples were digested in a dilute nitric acid solution (~40 wt%), then the mixture were filtered through 0.22 mm membrane filter. The metal ion containing filtrates were analyzed by inductive coupled plasma atomic emission spectroscopy (ICP-AES) (Optima 7000DV, PerkinElmer, USA). UV-vis spectra were obtained by using a UV-Vis spectrophotometer (Perkin Elmer Lambda 750). The surface charges of all the samples were measured by Zeta Potential Analyzer (ZetaPALS, Brookhaven Instruments, USA) based on electrophoretic mobility of the nanoparticles in aqueous media at pH=7.

Photocatalysis test

The photocatalytic degradation of orange (Ⅱ) was carried out in a 70 ml quartz reactor with 25 mg of as-synthesized sample and 50 mL of orange (Ⅱ) PBS solution (50 ppm, pH=7). The suspension was stirred in dark for 60 min to establish the adsorption equilibrium before the photocatalytic test started. Then, 300 W Xe lamp was used as the source of visible light using a cut-off filter of 420 nm to remove UV light. The catalysis sample was filtrated by a 0.22 μm PTFE syringe filter at settled time points. The concentrations of orange (Ⅱ) were monitored by

measuring the absorption intensity at maximum absorbance wavelength (λ=483 nm) using a UV-vis spectrophotometer. The photocatalytic performances of ZIF-8, MIL-125, MIL-125@ZIF-8 were compared based on the same dosages. The removal efficiency refers to the removal rate of dye from the original solution.

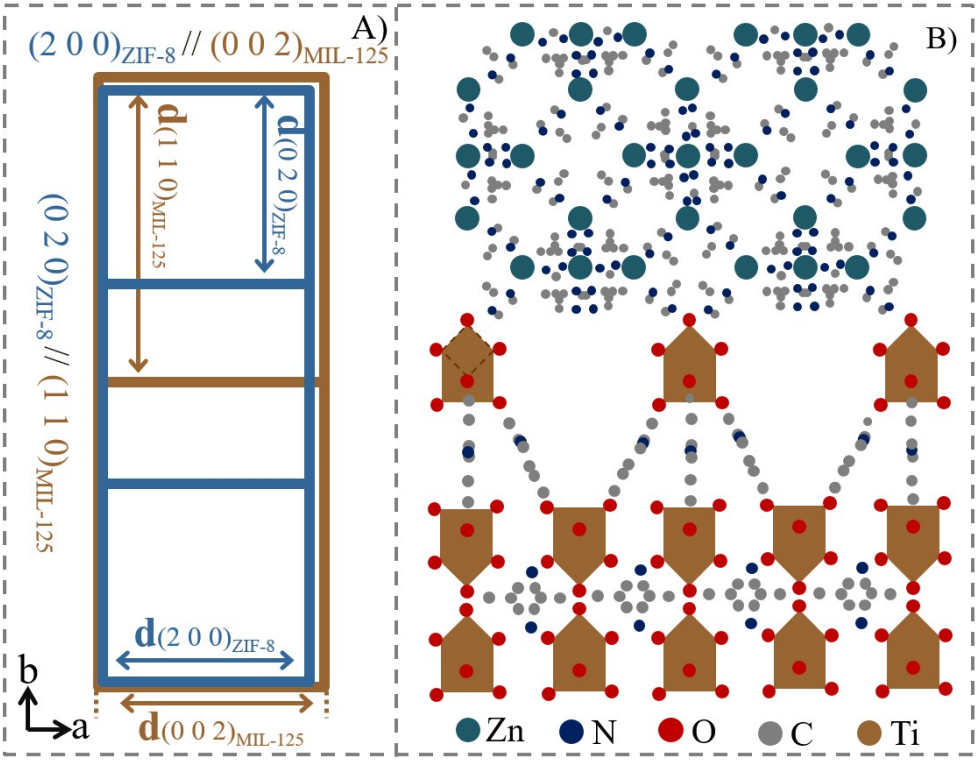

Scheme S1. (A) A schematic diagram showing the lattice mismatch in the $\{110\}_{MIL-125}$/ $\{001\}_{ZIF-8}$ interface; (B) A proposed overlaid molecular structure along b direction in (A) of the {110} face of MIL-125 and the {001} face of ZIF-8. The structures in (B) are proposed according to previous reports.[S3, S4]

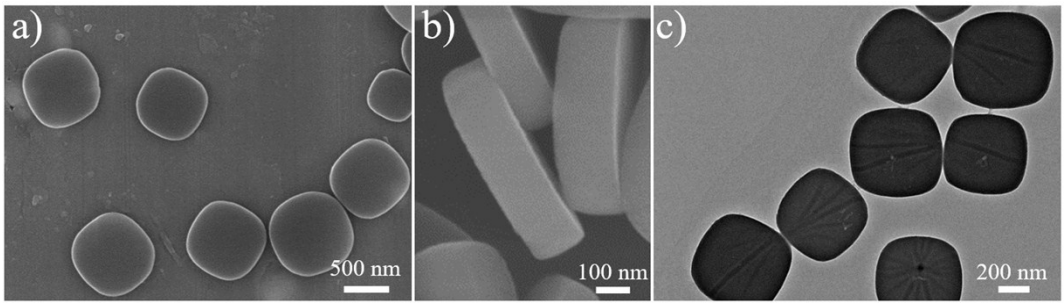

Figure S1. (a, b) SEM images and (c) TEM image of $_c$MIL-125.

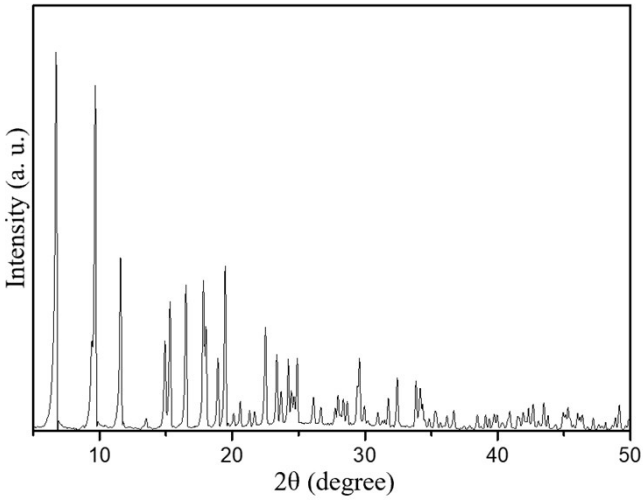

Figure S2. XRD pattern of $_c$MIL-125.

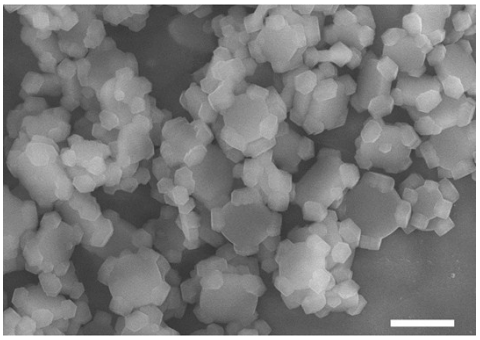

Figure S3. SEM image of $_c$MIL-125@ZIF-8 after sonication in methanol with frequency of 50 KHz for 10 min.

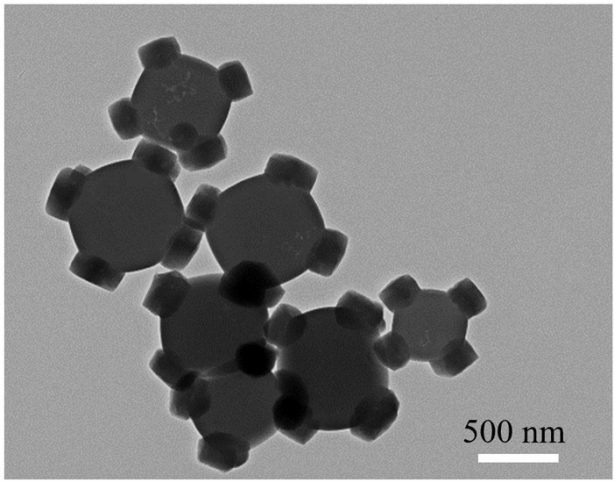

Figure S4. TEM image of $_c$MIL-125@ZIF-8.

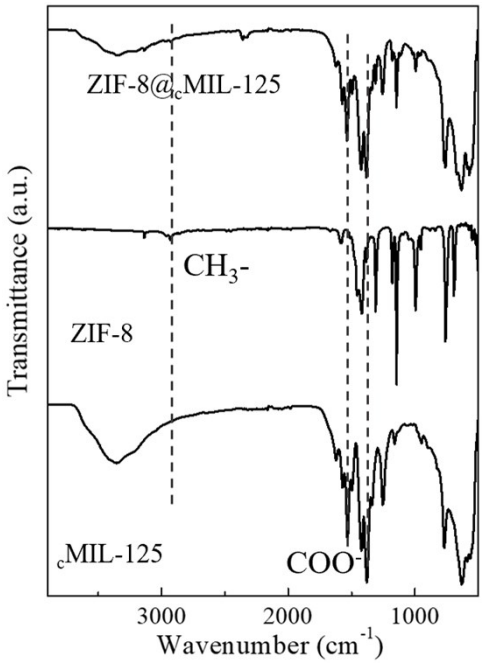

Figure S5. FT-IR spectra of ZIF-8, $_c$MIL-125, $_c$MIL-125@ZIF-8.

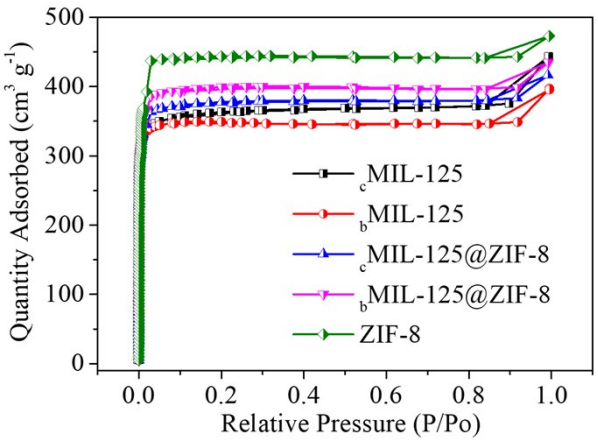

Figure S6. N_2 sorption curves of different samples.

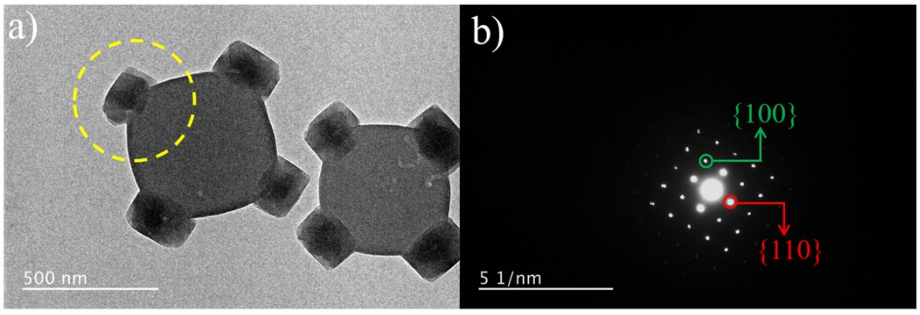

Figure S7. (a) TEM image and (b) SAED pattern in the marked region.

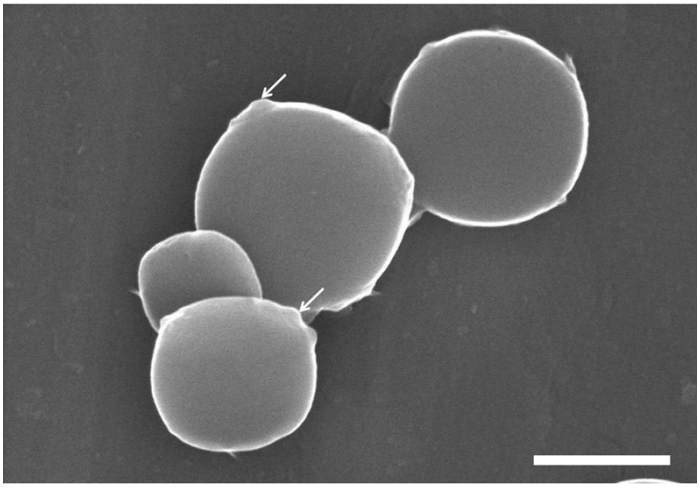

Figure S8. SEM image of sample after growth of ZIF-8 on $_{c}$MIL-125 for 2 min without methanol washing. The scale bar is 500 nm.

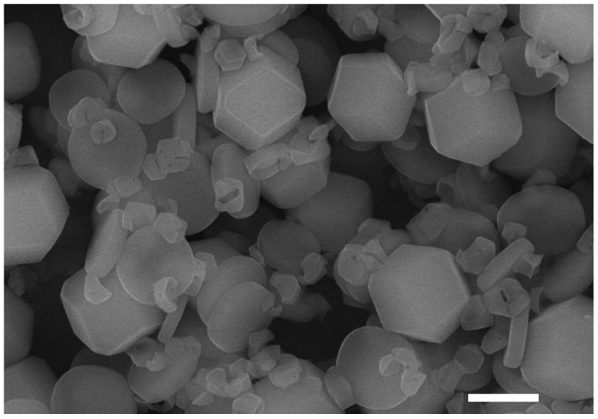

Figure S9. SEM image of sample by adding $_{c}$MIL-125 after growth of ZIF-8 for 2 min for pre-nucleation. The scale bar is 500 nm.

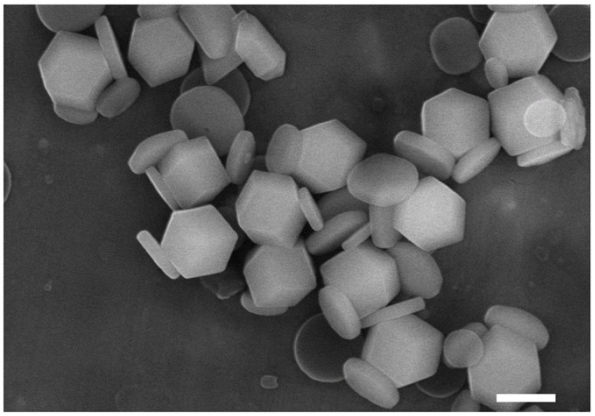

Figure S10. SEM image of sample by adding $_{c}$MIL-125 after growth of ZIF-8 for 5 min for pre-nucleation. The scale bar is 500 nm.

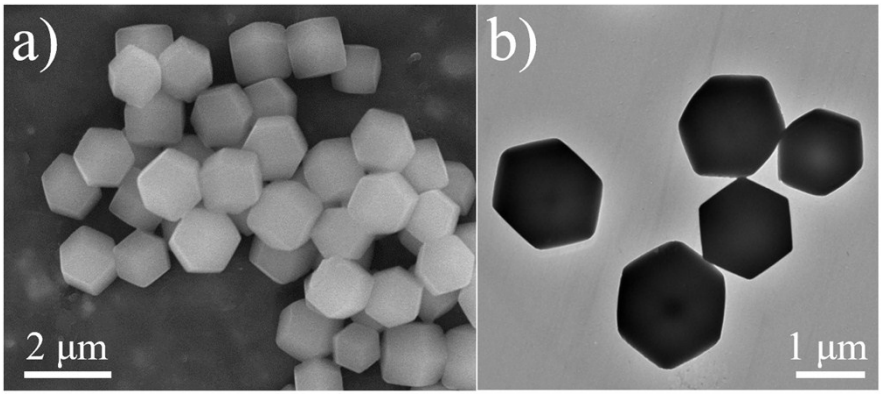

Figure S11. SEM and TEM images of ZIF-8 dodecahedron.

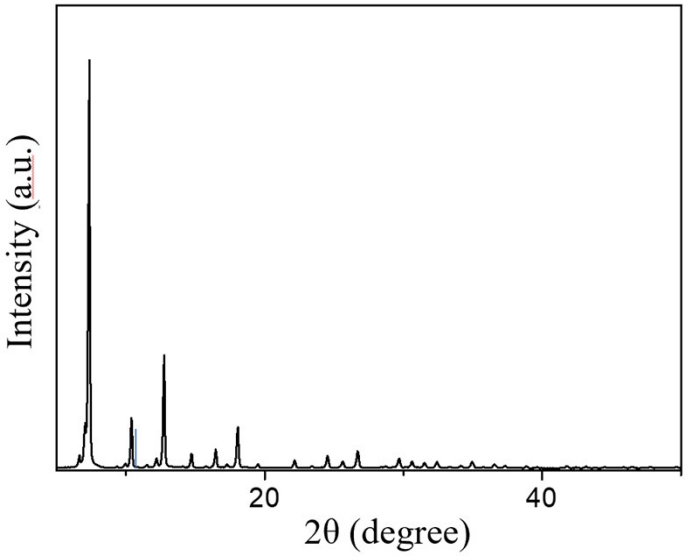

Figure S12. XRD pattern of ZIF-8 dodecahedron.

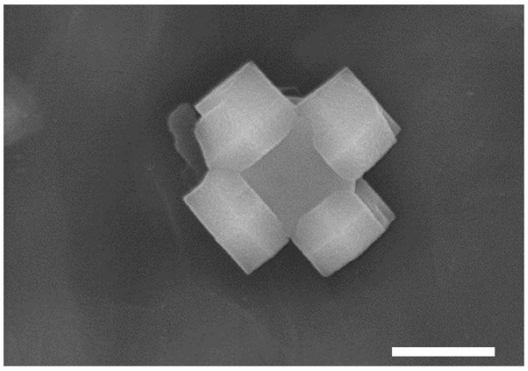

Figure S13. SEM image of $_c$MIL-125@ZIF-8 with larger ZIF-8 diameter. The scale bar is 500 nm.

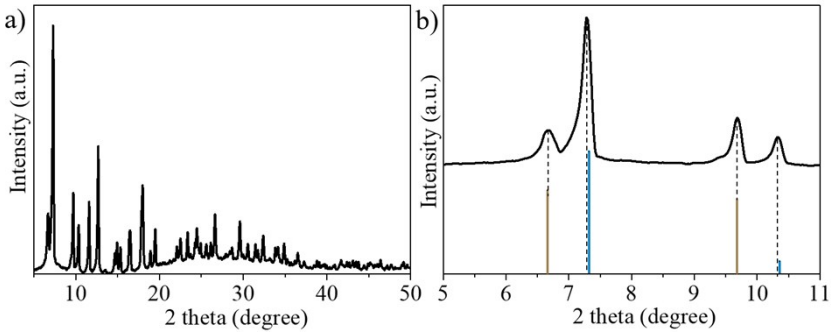

Figure S14. (a, b) XRD patterns of $_{c}$MIL-125@ZIF-8 with larger ZIF-8 diameter. (b) is the enlarged pattern of (a) in the range of 2θ from 5°-12°.

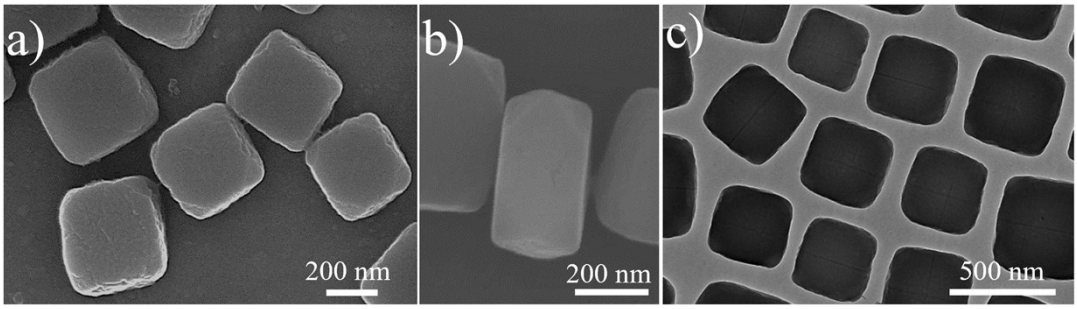

Figure S15. (a, b) SEM images and (c) TEM image of $_{b}$MIL-125.

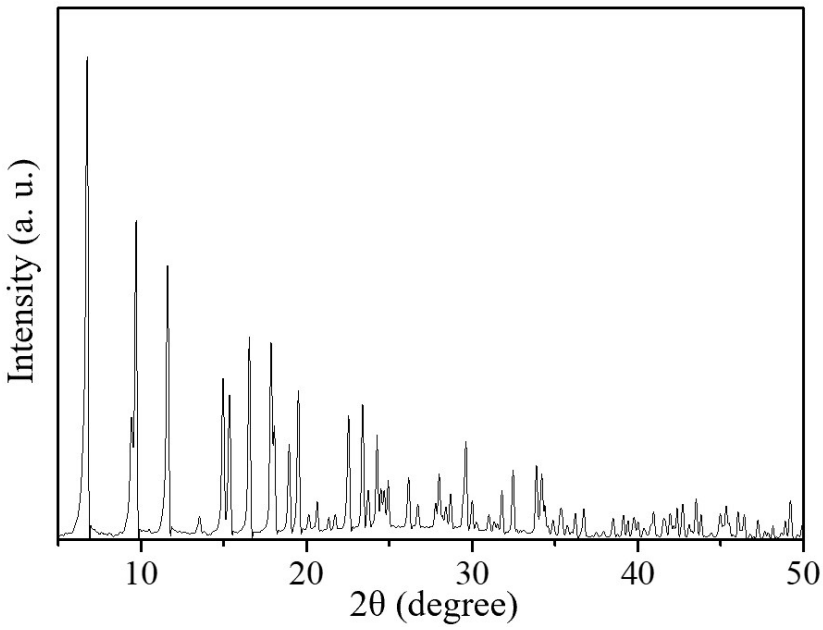

Figure S16. XRD pattern of $_b$MIL-125.

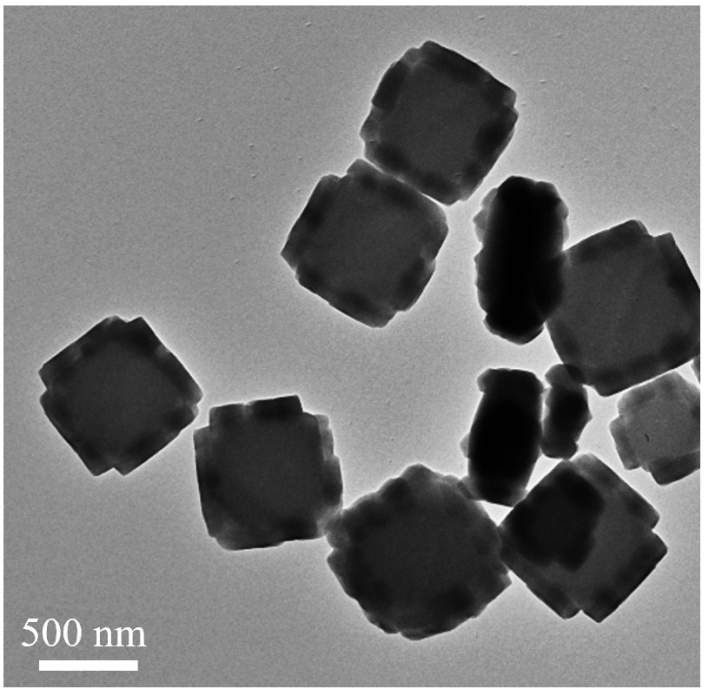

Figure S17. TEM image of $_b$MIL-125@ZIF-8.

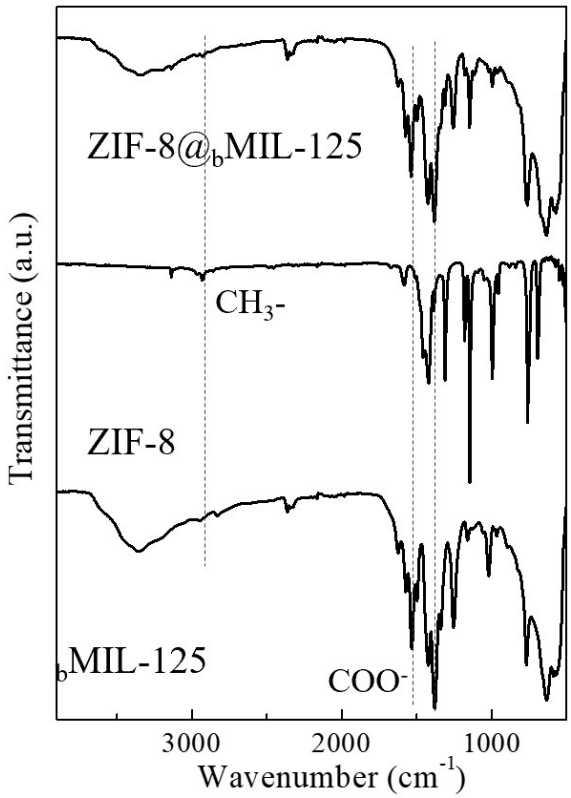

Figure S18. FT-IR spectra of ZIF-8, $_b$MIL-125, $_b$MIL-125@ZIF-8.

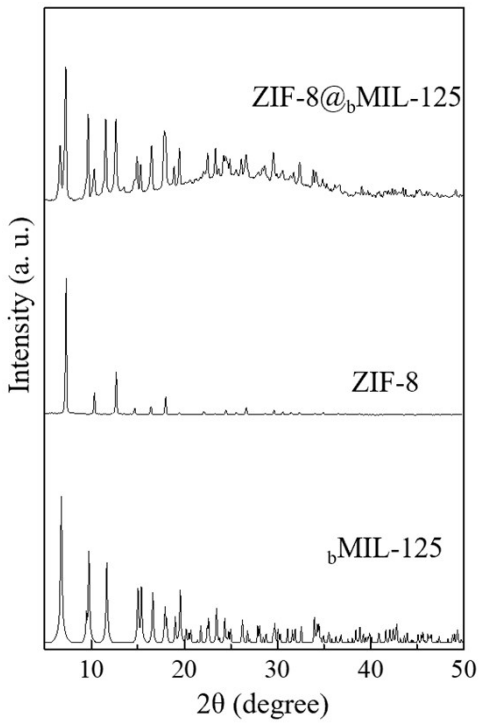

Figure S19. XRD pattern of $_b$MIL-125@ZIF-8.

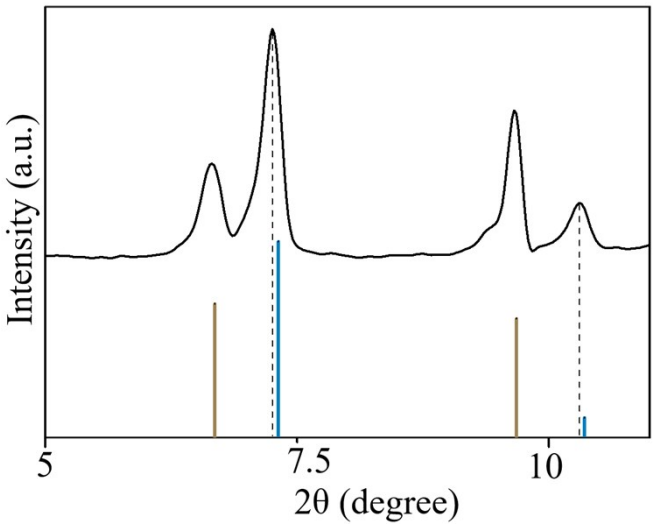

Figure S20. Enlarged XRD pattern of $_b$MIL-125@ZIF-8.

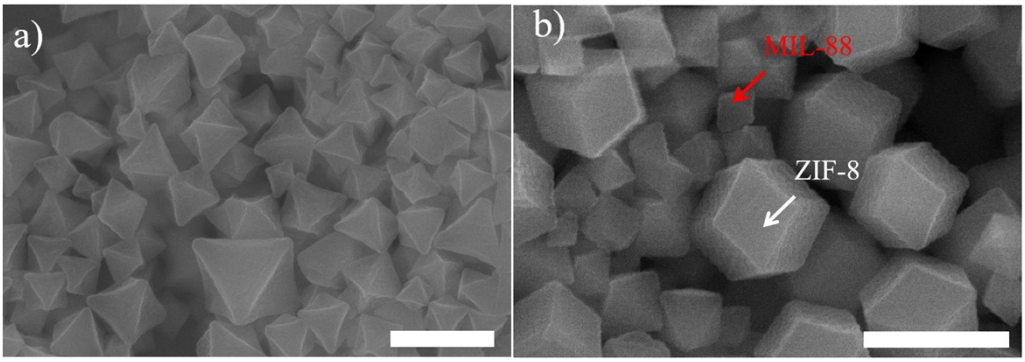

Figure S21. SEM images of (a) MIL-88B and (b) MIL-88B/ZIF-8. The scale bar is 500 nm.

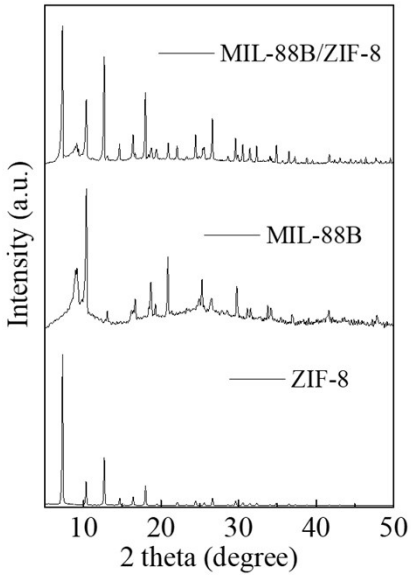

Figure S22. XRD patterns of ZIF-8, MIL-88B and MIL-88B/ZIF-8.

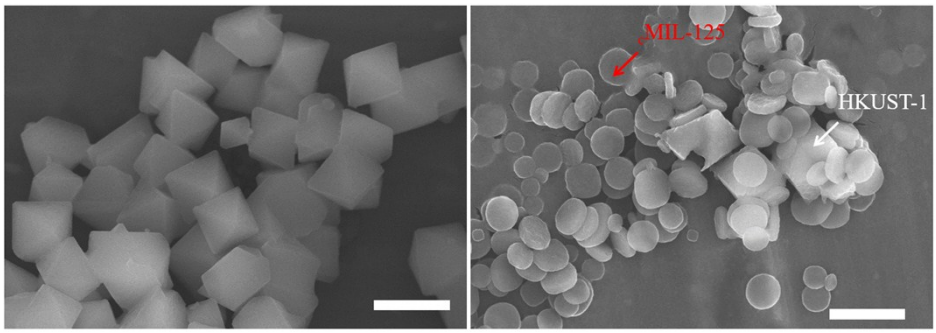

Figure S23. SEM images of (a) HKUST-1 and (b) $_{c}$MIL-125/HKUST-1. The scale bar is 2 μm.

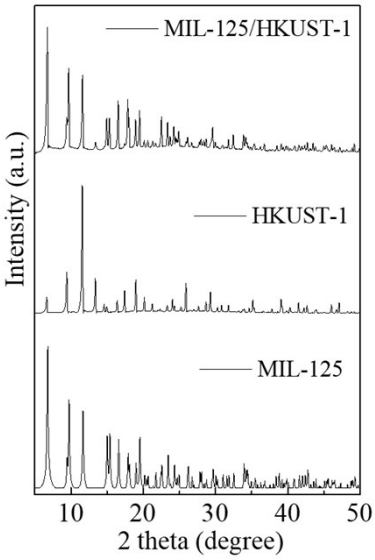

Figure S24. XRD patterns of MIL-125, HKUST-1 and $_{c}$MIL-125/HKUST-1.

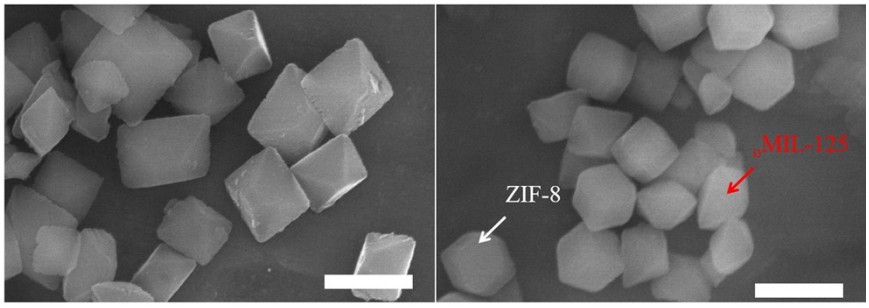

Figure 25. SEM images of (a) $_{o}$MIL-125 and (b) $_{o}$MIL-125/HKUST-1. The scale bar is 500 nm.

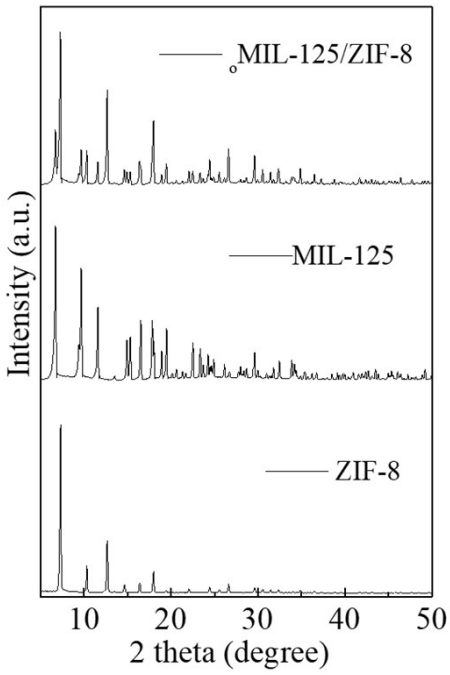

Figure S26. XRD patterns of ZIF-8, MIL-125 and $_{o}$MIL-125/ZIF-8.

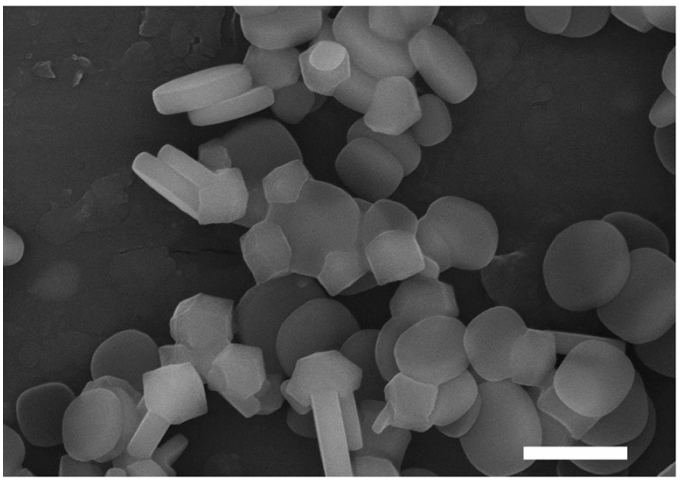

Figure S27. SEM image of sample obtained by adding Zn^{2+} first and then 2-MeIM. The scale bar is 1μm.

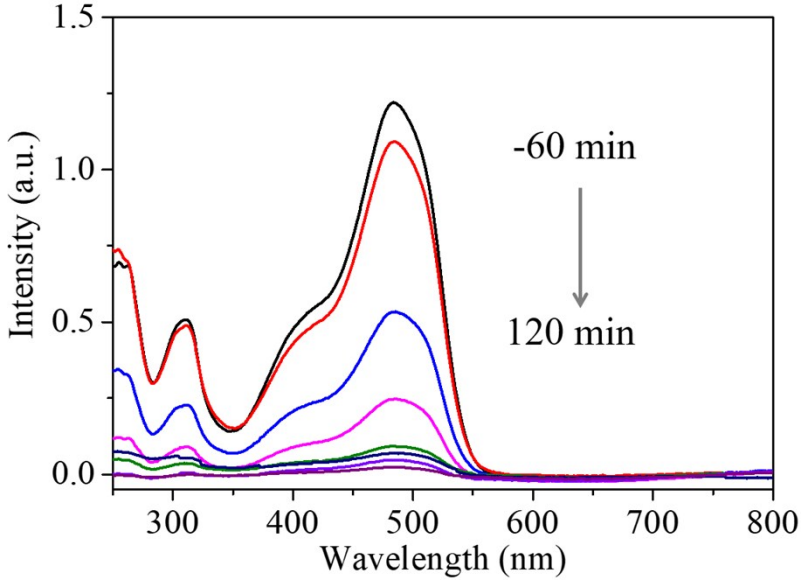

Figure S28. UV-vis spectra of supernatants during orange II degradation by $_c$MIL-125@ZIF-8.

The ultraviolet-visible (UV-vis) spectra (Figure S28) of supernatants during orange II degradation by $_c$MIL-125@ZIF-8 show that the intensity of peak at 483 nm corresponding to orange II gradually decreased with reaction processed, confirming the removal of orange II. Meanwhile, no new peaks are generated in the UV-vis spectra, indicating no other organic products generated or remained.

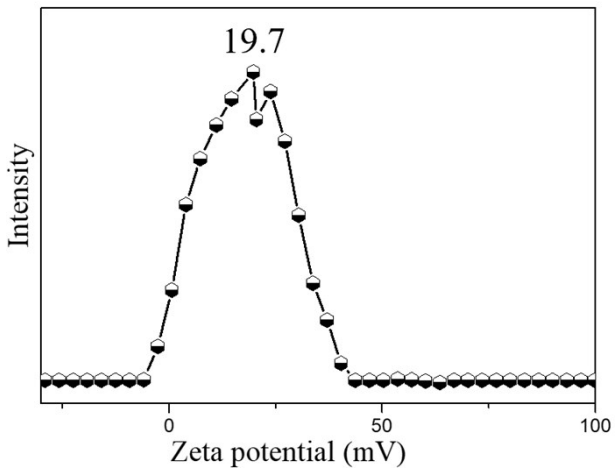

Figure S29. Zeta potentials of ZIF-8.

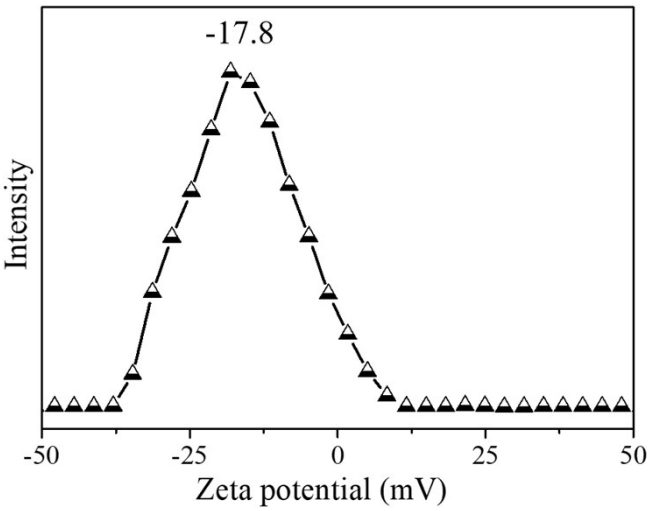

Figure S30. Zeta potentials of $_c$MIL-125.

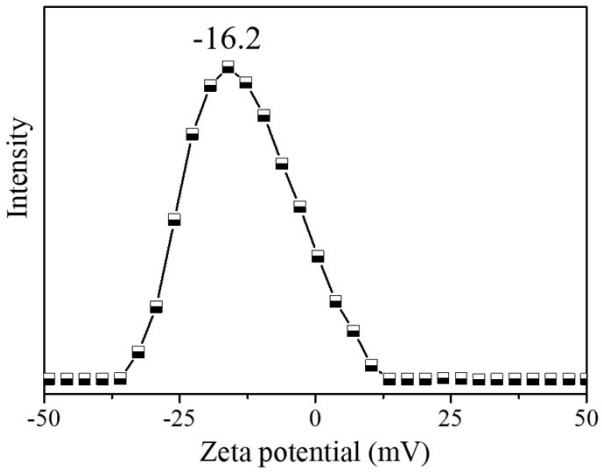

Figure S31. Zeta potentials of $_c$MIL-125.

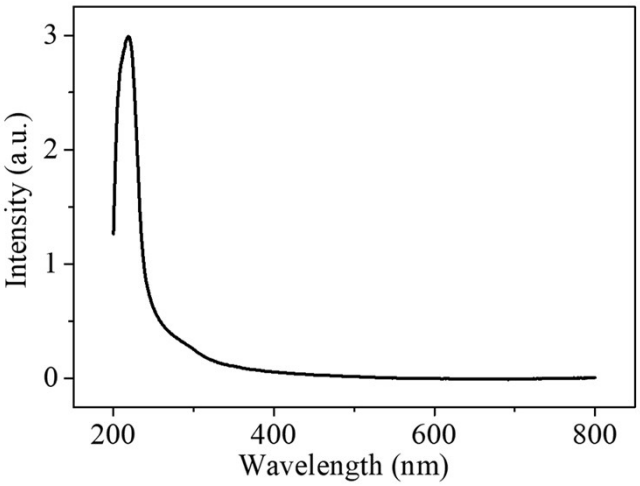

Figure S32. UV-vis spectra of ZIF-8.

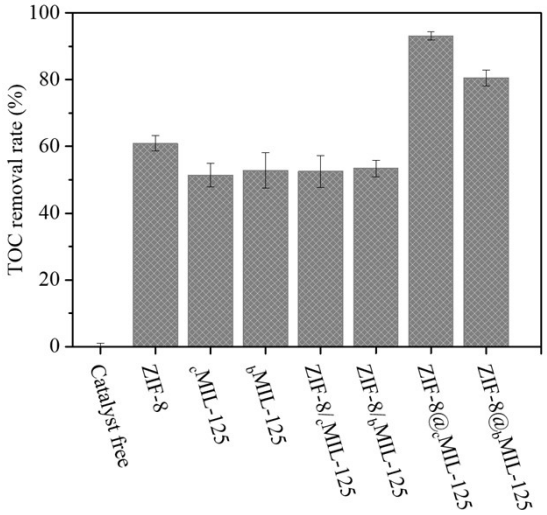

Figure S33. TOC removal rates of different catalysts.

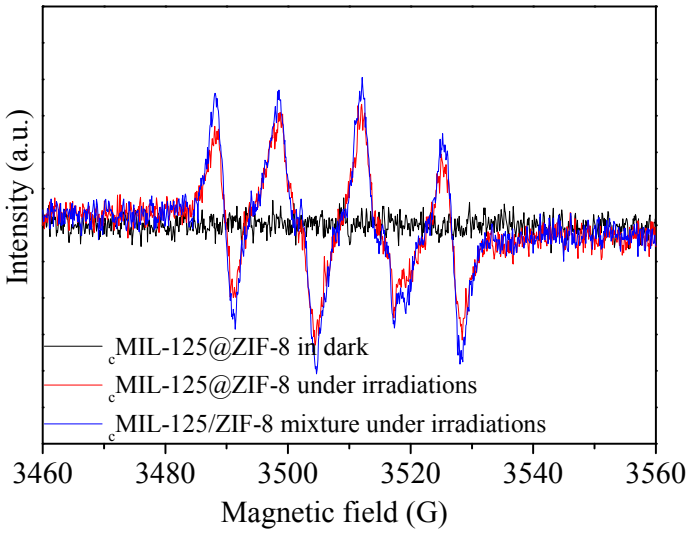

Figure S34. DMPO spin-trapping EPR spectra for superoxide radical detection of $_c$MIL-125@ZIF-8 in dark and $_c$MIL-125@ZIF-8 and $_c$MIL-125/ZIF-8 mixture in methanol under visible light irradiations.

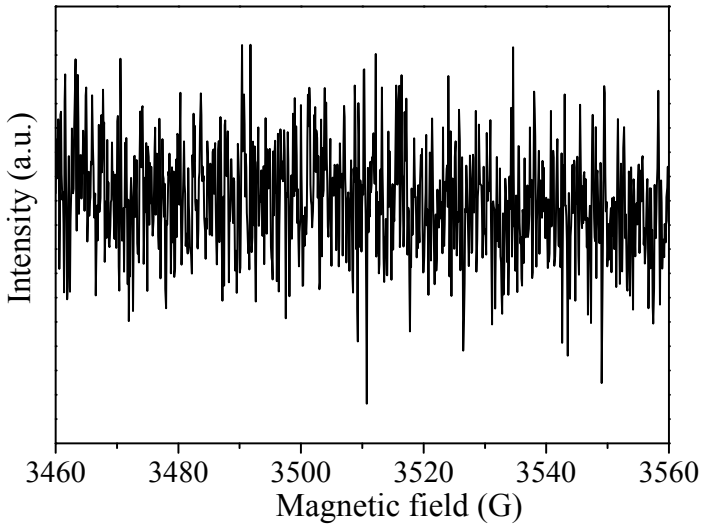

Figure S35. DMPO spin-trapping EPR spectra of $_{c}$MIL-125@ZIF-8 in water under visible light irradiations for detection of hydroxyl radical.

Table S1. Physical parameters of different samples

Samples	BET surface area/m^2 g^{-1}	Pore volume/cm^3 g^{-1}
$_{c}$MIL-125	1082.7	0.63
$_{b}$MIL-125	1063.9	0.59
$_{c}$MIL-125@ZIF-8	1236.9	0.67
$_{b}$MIL-125@ZIF-8	1171.7	0.65
ZIF-8	1339.1	0.73

References

(1) Hardi, M. Dan., Serre, C. Frot, T., Rozes, L. Maurin, G., Sanchez, C., Férey, G. A New Photoactive Crystalline Highly Porous Titanium (IV) Dicarboxylate. *J. Am. Chem. Soc.* **2009**, *131*, 10857.

(2) Khaletskaya, K., Pougin, A., Medishetty, R., Rösler, C., Wiktor, C., Strunk, J., Fischer, R. A. Fabrication of Gold/Titania Photocatalyst for CO_2 Reduction Based on Pyrolytic Conversion of the Metal-Organic Framework NH_2-MIL-125(Ti) Loaded with Gold Nanoparticles. *Chem. Mater.* **2015**, *27*, 7248.

(3) S. Z. Li, W. X. Shi, G. Lu, S. Z. Li, S. C. J. Loo, F. W. Huo, Unconventional Nucleation and Oriented Growth of ZIF-8 Crystals on Non-Polar Surface. Adv. Mater. 2012, 24, 5954.

(4) F. Guo, J. H. Guo, P. Wang, Y. S. Kang, Y. Liu, J. Zhao, W. Y. Sun, Facet-dependent photocatalytic hydrogen production of metal–organic framework NH_2-MIL-125(Ti). *Chem. Sci,* **2019**, 10, 4834.